JOURNAL OF NATURAL PRODUCTS

Article

pubs.acs.org/jnp

Polyketide Glycosides from *Bionectria ochroleuca* Inhibit *Candida albicans* Biofilm Formation

Bin Wang,[†,‡,§] Jianlan You,[†,‡,§] Jarrod B. King,[†,‡] Shengxin Cai,[†,‡] Elizabeth Park,[†,‡] Douglas R. Powell,[‡] and Robert H. Cichewicz*[,†,‡]

[†]Natural Product Discovery Group, Institute for Natural Products Applications and Research Technologies, and [‡]Department of Chemistry & Biochemistry, Stephenson Life Science Research Center, University of Oklahoma, 101 Stephenson Parkway, Norman, Oklahoma 73019, United States

Supporting Information

ABSTRACT: One of the challenges presented by *Candida* infections is that many of the isolates encountered in the clinic produce biofilms, which can decrease these pathogens' susceptibilities to standard-of-care antibiotic therapies. Inhibitors of fungal biofilm formation offer a potential solution to counteracting some of the problems associated with *Candida* infections. A screening campaign utilizing samples from our fungal extract library revealed that a *Bionectria ochroleuca* isolate cultured on Cheerios breakfast cereal produced metabolites that blocked the *in vitro* formation of *Candida albicans* biofilms. A scale-up culture of the fungus was undertaken using mycobags (also known as mushroom bags or spawn bags), which afforded four known [TMC-151s C−F (**1**−**4**)] and three new [bionectriols B−D (**5**−**7**)] polyketide glycosides. All seven metabolites exhibited potent biofilm inhibition against *C. albicans* SC5314, as well as exerted synergistic antifungal activities in combination with amphotericin B. In this report, we describe the structure determination of the new metabolites, as well as compare the secondary metabolome profiles of fungi grown in flasks and mycobags. These studies demonstrate that mycobags offer a useful alternative to flask-based cultures for the preparative production of fungal secondary metabolites.

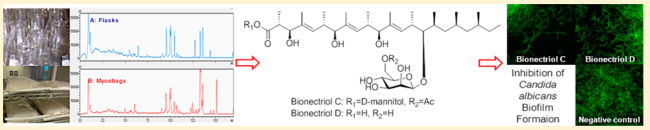

Opportunistic *Candida* infections pose a significant health burden to immunocompromised patients, as well as healthy adult women.[1] According to the Centers for Disease Control (CDC), approximately 7% of infants, 31% those suffering from AIDS, and 20% of cancer patients undergoing chemotherapy develop oral candidiasis.[1] Even more common is vulvovaginal candidiasis, which is estimated to occur one or more times in 75% of women who are otherwise healthy.[1] A major obstacle to effectively treating these infections is that many clinical *Candida* isolates form biofilms that afford resistance against a variety of antifungal drugs including amphotericin B.[2−4] Therefore, inhibitors and/or agents that disrupt fungal biofilms could provide an effective means for helping control *Candida* infections. Since 2011, our group has engaged in a screening effort to detect metabolites that inhibit the formation of *Candida albicans* biofilms. This has led to several discoveries including waikialoid A,[5] mutanobactins,[6] and shearinines.[7]

A consistent challenge associated with the preparation of secondary metabolites from fungi is that under many laboratory culture conditions fungi produce restricted sets of natural products that represent only a fraction of their overall biosynthetic potential. Informal observations suggest that in many cases the switch from broth-based to solid-phase fermentation conditions may lead to the generation of more chemically diverse secondary metabolite profiles.[5,8] Recently, our group introduced an unconventional solid-phase cultivation approach employing Cheerios breakfast cereal as the fermentation medium. A series of several early successes using this method[9,10] has spurred our interests in extending its application to include a broader range of fungal isolates.

Employing this solid-phase culture method, a small-scale extract of *Bionectria ochroleuca* was identified that inhibited *C. albicans* biofilm formation. Assay-guided purification yielded seven bioactive polyketide glycosides including three new metabolites, bionectriols B−D (**5**−**7**). Compounds **5**−**7** exhibit structural similarities to other compounds in this metabolite family, which include TMC-151s,[11,12] bionectriol A,[13] roslipin,[14,15] and cladionol.[16] In this paper, we report the purification of several known and new natural products bearing an *O*-linked glycosylated polyketide scaffold, as well as demonstrate that these compounds inhibit *C. albicans* biofilm formation. As an additional element of our investigation, we explored the application of mycobags (commonly referred to as mushroom bags or spawn bags) as a convenient high-surface-area container for the cultivation of fungi. Our studies demonstrate that mycobags are effective tools for the scale-up preparation of fungi, yielding profiles that are similar to those obtained for solid-phase fungal cultures grown in traditional Erlenmeyer flasks.

Received: June 30, 2014
Published: October 10, 2014

dx.doi.org/10.1021/np500531j | *J. Nat. Prod.* 2014, 77, 2273−2279

Chart 1

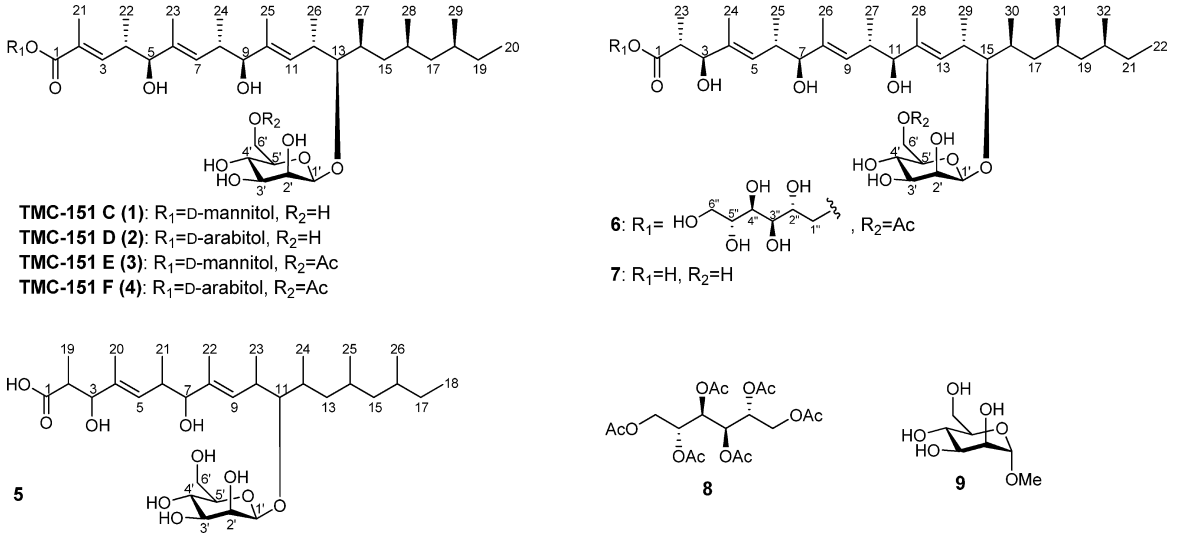

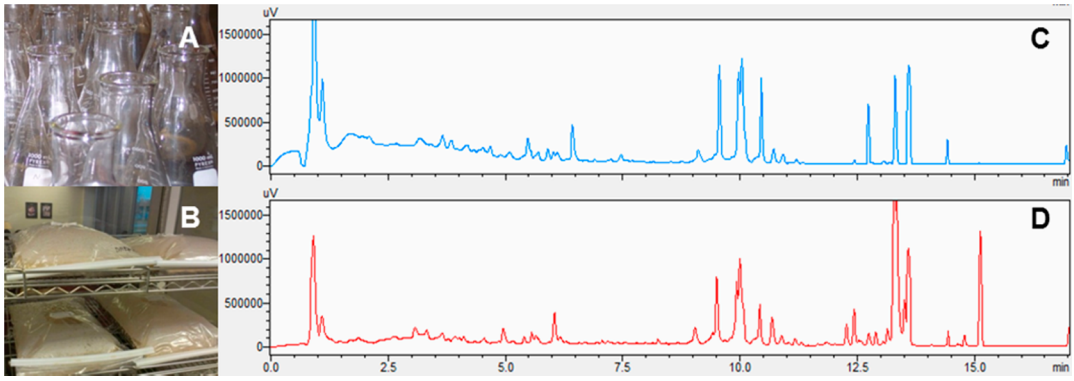

Figure 1. Effects of different culture vessels on the secondary metabolome of *B. ochroleuca* grown on a Cheerios-based medium. The *B. ochroleuca* cultures were grown in 1 L Erlenmeyer flasks (A) or mycobags (B). The resulting secondary metabolome profiles (PDA detection at 200−400 nm) from the flask-derived (C) and mycobag-derived (D) cultures reveal relatively modest changes in their respective metabolite composition.

RESULTS AND DISCUSSION

Fungal isolate BVK-SMA-2 was obtained from a soil sample collected in Buffalo Valley, Oklahoma. A BLAST analysis of its ITS sequence data demonstrated that the isolate was 99% identical to *B. ochroleuca*. For the purpose of comparing its growth and metabolite profiles using two solid-phase culturing techniques, the *B. ochroleuca* was inoculated onto Cheerios breakfast cereal in (a) 50 × 1 L Erlenmeyer flasks and (b) 3 mycobags (each 53 cm × 35 cm). The amounts of Cheerios and inoculum introduced into the mycobags and flasks were scaled relative to one another in order to ensure the ratios of inoculum to culturable surface area in the two types of vessels were approximately equivalent. Both sets of cultures were incubated at 25 °C under identical lighting for 4 weeks. The secondary metabolites from both sets of *B. ochroleuca* cultures were extracted with EtOAc for chemical analysis and biological testing.

Extracts were dissolved in MeOH−H_2O (9:1), and the supernatants were subject to LC-PDA-ESIMS analysis. The resulting metabolite profiles for both sets of *B. ochroleuca* cultures were judged to be similar (Figure 1). As an extension of this observation, the secondary metabolite profiles for several other fungi grown under both types of solid-phase culture conditions were also compared (Figure S1). In the majority of cases, the fungi exhibited remarkably similar metabolite profiles, indicating that mycobags are a suitable alternative to flask-based fermentation. Significantly, the culturable surface area of one mycobag (1855 cm^2) is equivalent to that of approximately 18 × 1 L Erlenmeyer flasks. Considering that mycobags are relatively inexpensive (~0.50−0.60 USD/bag with one hydrophobic gas exchange patch), occupy limited vertical space (mycobags can be incubated in a relatively flattened position), and require no cleaning (mycobags are disposed of after autoclaving), their use for solid-phase fungal cultures presents many advantages.

After comparing the *B. ochroleuca* secondary metabolomes generated under both sets of conditions, the extracts were pooled, and the bioactive compounds were purified using normal-phase, size-exclusion, and reversed-phase chromatography methods to yield four known *O*-linked glycosylated polyketides, TMC-151s C−F (**1**−**4**), and three new metabolites, named bionectriols B−D (**5**−**7**). Metabolites **1**−**4** were identified by comparisons of their MS data, ^1H and ^{13}C NMR spectra, and optical rotation values to published values.[11]

Compound **5** was obtained as a colorless, amorphous solid that yielded an adduct ion with *m*/*z* 625.3934 $[M + Na]^+$ under HRESIMS conditions, which was determined to represent the molecular formula $C_{32}H_{58}O_{10}Na$ (calcd 625.3928, Δ 0.96 ppm). The ^1H, ^{13}C, and HSQC NMR data (Table 1) suggested

dx.doi.org/10.1021/np500531j | J. Nat. Prod. 2014, 77, 2273−2279

Table 1. NMR Data for Compounds 5−7[a] (δ in ppm, methanol-d_4)

	5		6		7	
carbon	δ_C, type	δ_H (m, J in Hz)	δ_C, type	δ_H (m, J in Hz)	δ_C, type	δ_H (m, J in Hz)
1	179.9, qC		177.8, qC		181.5, qC	
2	44.7, CH	2.54 (m)	44.7, CH	2.68 (m)	45.2, CH	2.49 (m)
3	81.8, CH	4.05 (d, 9.7)	82.1, CH	4.08 (d, 10.0)	82.0, CH	4.02 (d, 9.5)
4	136.2, qC		135.9, qC		136.8, qC	
5	135.1, CH	5.33 (d, 9.1)	135.3, CH	5.36 (d, 9.2)	134.1, CH	5.34 (d, 9.6)
6	37.1, CH	2.62 (m)	36.6, CH	2.65 (m)	36.7, CH	2.65 (m)
7	84.3, CH	3.71 (d, 9.1)	84.3, CH	3.72 (d, 9.0)	83.9, CH	3.72 (d, 8.6)
8	134.7, qC		137.2, qC		137.5, qC	
9	134.8, CH	5.54 (d, 9.5)	134.3, CH	5.29 (d, 9.3)	133.6, CH	5.30 (d, 8.9)
10	36.2, CH	2.74 (m)	36.9, CH	2.61 (m)	37.1, CH	2.61 (m)
11	87.3, CH	3.48 (dd, 6.3, 3.5)	84.6, CH	3.64 (m)	84.4, CH	3.68 (d, 9.1)
12	34.2, CH	1.86 (m)	134.7, qC		134.9, qC	
13	43.9, CH_2	0.99, 1.40 (m, m)	135.0, CH	5.52 (d, 9.5)	134.7, CH	5.55 (d, 9.2)
14	28.8, CH	1.62 (m)	36.1, CH	2.73 (m)	36.2, CH	2.74 (m)
15	46.0, CH_2	0.91, 1.25 (m, m)	87.4, CH	3.43 (dd, 6.4, 3.2)	87.1, CH	3.49 (dd, 6.4, 3.5)
16	32.9, CH	1.44 (m)	34.3, CH	1.85 (m)	34.2, CH	1.85 (m)
17	29.9, CH_2	1.08, 1.41 (m, m)	43.9, CH_2	0.99, 1.40 (m, m)	43.9, CH_2	0.98, 1.39 (m, m)
18	11.5, CH_3	0.89 (d, 6.3)	28.8, CH	1.62 (m)	28.8, CH	1.62 (m)
19	15.0, CH_3	0.97 (d, 7.2)	46.1, CH_2	0.92, 1.25 (m, m)	46.1, CH_2	0.90, 1.26 (m, m)
20	10.8, CH_3	1.64 (br s)	32.9, CH	1.45 (m)	32.9, CH	1.45 (m)
21	17.8, CH_3	0.78 (d, 6.8)	29.9, CH_2	1.10, 1.42 (m, m)	29.9, CH_2	1.08, 1.38 (m, m)
22	11.3, CH_3	1.64 (br s)	11.5, CH_3	0.88 (m)	11.6, CH_3	0.87 (m)
23	18.6, CH_3	0.99 (d, 6.9)	14.7, CH_3	0.98 (d, 7.0)	15.2, CH_3	0.96 (d, 6.8)
24	15.5, CH_3	0.95 (d, 6.8)	10.7, CH_3	1.63 (br s)	10.9, CH_3	1.64 (br s)
25	21.3, CH_3	0.89 (d, 6.3)	17.7, CH_3	0.79 (d, 6.8)	17.8, CH_3	0.80 (d, 6.8)
26	20.7, CH_3	0.89 (d, 6.3)	11.4, CH_3	1.67 (br s)	11.5, CH_3	1.67 (br s)
27			17.8, CH_3	0.75 (d, 6.7)	17.8, CH_3	0.77 (d, 6.8)
28			11.1, CH_3	1.64 (br s)	11.3, CH_3	1.64 (br s)
29			18.7, CH_3	0.97 (d, 7.2)	18.6, CH_3	0.98 (d, 6.9)
30			15.5, CH_3	0.94 (d, 7.1)	15.5, CH_3	0.94 (d, 6.5)
31			21.2, CH_3	0.89 (d, 6.2)	21.3, CH_3	0.89 (d, 6.3)
32			20.7, CH_3	0.89 (d, 6.2)	20.7, CH_3	0.89 (d, 6.3)
1′	102.6, CH	4.47 (br s)	102.7, CH	4.46 (br s)	102.5, CH	4.49 (br s)
2′	72.7, CH	3.89 (d, 2.8)	72.4, CH	3.91 (d, 3.0)	72.7, CH	3.89 (d, 2.8)
3′	75.7, CH	3.37 (dd, 9.5, 3.2)	75.5, CH	3.39 (dd, 9.6, 3.1)	75.7, CH	3.37 (dd, 9.5, 3.1)
4′	68.5, CH	3.58 (dd, 9.5, 9.4)	68.9, CH	3.51 (dd, 9.6, 9.6)	68.4, CH	3.58 (dd, 9.6, 9.5)
5′	78.3, CH	3.15 (m)	75.7, CH	3.36 (m)	78.3, CH	3.15 (m)
6′	62.9, CH_2	3.75 (dd, 11.6, 5.2)	65.6, CH_2	4.26 (dd, 11.8, 7.2)	62.9, CH_2	3.77 (dd, 11.6, 5.2)
		3.87 (dd, 11.1, 2.1)		4.41 (dd, 11.9, 1.7)		3.87 (dd, 11.0, 1.9)
7′			172.8, qC			
8′			21.0, CH_3	2.09 (s)		
1″			68.0, CH_2	4.20 (dd, 11.5, 6.1)		
				4.47 (dd, 11.3, 2.4)		
2″			70.4, CH	3.91 (m)		
3″			71.1, CH	3.82 (m)		
4″			71.0, CH	3.80 (m)		
5″			72.9, CH	3.69 (m)		
6″			65.2, CH_2	3.64, 3.82 (m, m)		

[a]Assignments based on ^{1}H, ^{13}C, and HSQC NMR (^{13}C 100/^{1}H 400 MHz) experiments at room temperature.

the presence of nine methyl, three methylene, six methine, one oxygenated methylene, eight oxygenated methine, and four olefinic carbons. The HMBC spectrum displayed a correlation from H_3-19 to C-1, indicating the presence of an ester carbonyl carbon that had not been detected in the ^{13}C spectrum. The other features of the ^{13}C spectrum of **5** were similar to those for **1**, except that the sugar alcohol moiety and one propenyl subunit (equivalent to C-2, C-3, and C-21 in **1**) were missing (Figure S5). The carbon chemical shifts at δ_C 62.9, 68.5, 72.7, 75.7, 78.3, and 102.6 denoted the presence of a hexopyranose. An HMBC correlation from H-1′ to C-11 indicated that the hexopyranose moiety was attached to C-11. Additional HMBC correlations that were critical for verifying the planar structure of **5** are illustrated in Figure 2. On the basis of 2D ROESY correlations between H_3-20 and H-6, as well as H_3-22 and H-10 (Figure 2), both the C-4−C-5 and C-8−C-9 olefins were determined to be *E*-configured.

dx.doi.org/10.1021/np500531j | J. Nat. Prod. 2014, 77, 2273−2279

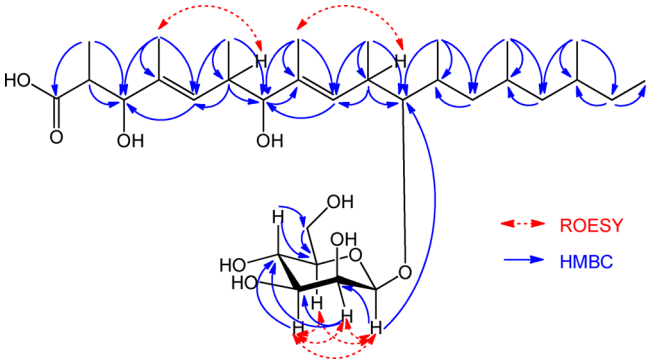

Figure 2. Key HMBC and ROESY correlations for **5**.

The relative configuration of the glycan moiety was ascertained based on gated decoupling and ROESY NMR experiments. In the gated decoupling experiment (Figure S6), the coupling constant between the anomeric carbon and hydrogen atoms was determined to be $^{1}J_{C\text{-}1',H\text{-}1'}$ = 154.5 (<160), indicating a β-orientation.[17] ROESY correlations between H-1′ and H-2′, H-1′ and H-3′, H-1′ and H-5′, H-2′ and H-3′, H-2′ and H-5′, and H-3′ and H-5′ were observed (Figure 2), which were consistent with a mannose moiety. Additional comparisons between our carbon chemical shift data (C-1′ to C-6′) and those published for similar compounds[11] further corroborated this assignment. Further efforts to address the absolute configuration of the presumably polyketide portion of the metabolite proved unsuccessful; thus the absolute configuration of the aglycan component of **5** was not determined.

Compound **6** was obtained as a colorless, amorphous solid. The HRESIMS data for **6** provided an adduct ion $[M + Na]^+$ at m/z 929.5474, which represented the molecular formula $C_{46}H_{82}O_{17}Na$ (calcd 929.5450, Δ 2.58 ppm). The ^{1}H, ^{13}C, and HSQC NMR spectra (Table 1) suggested the presence of 12 methyl, three methylene, seven methine, three oxygenated methylene, 13 oxygenated methine, six olefinic, and two ester carbonyl carbons. The ^{13}C NMR spectrum of **6** was similar to that of **3** with the major exceptions being the presence of additional methyl (δ_C 14.7), methine (δ_C 44.7), and oxygenated methine (δ_C 82.1) groups (Figures S13 and S14). HMBC correlation data were employed to deduce the planar structure of **6**, which revealed that the new carbons were located adjacent to the C-1 ester. A ROESY experiment was performed revealing correlations between H_3-24 and H-6, H_3-26 and H-10, and H_3-28 and H-14, thus verifying that the olefins were *E*-configured. In addition, correlations between H-1′ and H-2′, H-1′ and H-3′, H-1′ and H-5′, H-2′ and H-3′, H-2′ and H-5′, and H-3′ and H-5′ were detected, indicating that the glycan was a mannose. A coupling constant of $^{1}J_{C\text{-}1',H\text{-}1'}$ = 154.1 was observed for the anomeric C−H bond supporting a β-orientation.

Further efforts to substantiate the absolute configurations of mannose and mannitol in **6** were pursued using a modification of Kohno's approach.[11] Compound **6** was hydrolyzed in 0.4 M NaOH, the reaction mixture was neutralized, and products were partitioned against EtOAc to yield **7**. The water layer was dried under vacuum and reacted with Ac_2O in anhydrous pyridine, and the products were extracted with EtOAc to yield **8**, hexa-*O*-acetylmannitol (Figures S29, S30). A comparison of the optical rotation values for **8** ($[\alpha]_D^{25}$ +24 [*c* 0.13, $CHCl_3$]) and authentic hexa-*O*-acetyl-D-mannitol ($[\alpha]_D^{25}$ +26 [*c* 0.693, $CHCl_3$]) suggested **8** was D-configured.

Another new metabolite was purified from the fungal crude extract; however, its HRESIMS, 1D and 2D NMR (Figures S21−27), and optical rotation data were identical to those of the base-hydrolysis product **7**. Compound **7** was subjected to acid hydrolysis in 1 M methanolic HCl at 70 °C and extracted with EtOAc. The water layer was neutralized and dried under vacuum to yield **9**, which was determined to be methyl-α-mannopyranoside based upon comparisons of its ^{13}C NMR spectrum (δ 102.7, 72.0, 72.5, 68.4, 74.4, 62.7, and 55.2, Figure S32) with published data.[18] A comparison of the optical rotation value for **9** ($[\alpha]_D^{25}$ +60 [*c* 0.09, H_2O]) with authentic methyl-α-D-mannopyranoside ($[\alpha]_D^{25}$ +80 [*c* 10, H_2O]) suggested that **9** is D-configured. During the course of these studies, colorless, needle-like crystals of **7** were fortuitously obtained from a concentrated methanol solution of the metabolite. This provided an opportunity to use X-ray diffraction analysis to verify the planar structure of **7**, as well as assign its absolute configuration (Figure S31). Results from the X-ray experiment revealed the absolute configuration of **2***R*,**3***S*,**6***S*,**7***S*,**10***S*,**11***S*,**14***S*,**15***R*,**16***S*,**18***S*,**20***S*.

Compounds **3**, **4**, and **6** produced modest inhibition of *C. albicans* cell growth with IC_{50} values of 36.3 ± 11.3, 41.0 ± 5.6, and 24.1 ± 4.5 μM (30.8 ± 9.6, 33.6 ± 4.6, and 21.8 ± 4.1 μg/mL), respectively. The biofilm-inhibiting positive control ETYA (5,8,11,14-eicosatetraynoic acid) and all of the other purified metabolites were inactive in this assay at concentrations of up to 100 μM. However, all the compounds exhibited biofilm inhibition properties with IC_{50} values ranging from 1.1 to 5.0 μM (0.9 to 3.0 μg/mL), and most of them displayed increased inhibition relative to ETYA (Table 2, Figure 4). The potencies

Table 2. Inhibition of *C. albicans* SC5314 Biofilm Formation and Growth with Compounds 1−7

compound	IC_{50}[a] for biofilm inhibition, μM (μg/mL)	IC_{50} for growth inhibition, μM (μg/mL)
1	1.1 ± 0.7 (0.9 ± 0.6)	>100 (81)
2	1.5 ± 0.1 (1.2 ± 0.1)	>100 (78)
3	1.5 ± 0.1 (1.3 ± 0.1)	36.3 ± 11.3 (30.8 ± 9.6)
4	1.2 ± 0.5 (1.0 ± 0.4)	41.0 ± 5.6 (33.6 ± 4.6)
5	5.0 ± 2.4 (3.0 ± 1.4)	>100 (60)
6	1.5 ± 0.2 (1.4 ± 0.2)	24.1 ± 4.5 (21.8 ± 4.1)
7	2.4 ± 0.0 (1.7 ± 0.0)	>100 (70)
ETYA	3.4 ± 0.0 (1.2 ± 0.0)	>100 (30)

[a] IC_{50} values are expressed as the concentrations corresponding to 50% of the maximum biofilm formation.

of the *B. ochroleuca*-derived biofilm inhibitors are similar to waikialoid A (IC_{50} value of 1.4 μM),[5] yet are 2 to 5 times more potent than the mutanobactins and shearinines.[6,7] All of the compounds were tested for their abilities to synergistically enhance the activity of amphotericin B against *C. albicans*. FICI

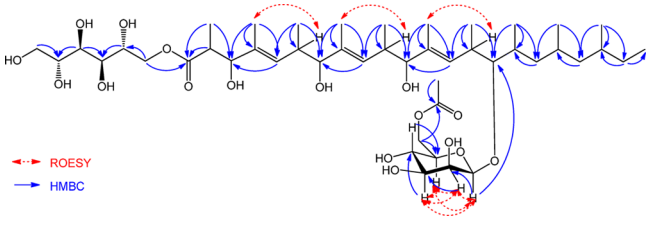

Figure 3. Key HMBC and ROESY correlations for **6**.

dx.doi.org/10.1021/np500531j | J. Nat. Prod. 2014, 77, 2273−2279

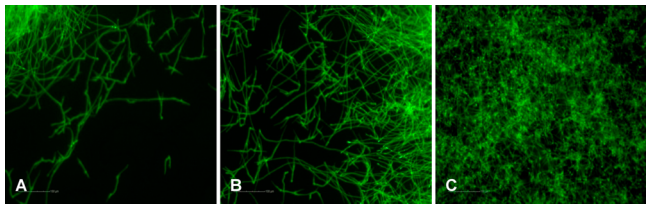

Figure 4. Effects of compounds **6** and **7** (2.5 μM) on *C. albicans* SC5314 biofilm formation. The *C. albicans* cultures were prepared in RMPI 1640-MOPS medium and treated with compounds **6** (A), **7** (B), or DMSO vehicle (C) before incubating at 37 °C for 48 h. Panels A–C illustrate representative fluorescent images taken from triplicate cultures.

(fractional inhibitory concentration index) values for all seven compounds were found to be <0.5, indicating synergistic effects with amphotericin B. All of the compounds were found to enhance the potency of amphotericin B up to 4-fold (Table 3).

EXPERIMENTAL SECTION

General Experimental Procedures. UV data were recorded on a Hewlett-Packard 8452A diode array spectrophotometer. Optical rotation measurements were made on an AUTOPOL III automatic polarimeter. NMR spectra were obtained on a Varian Unity Inova spectrometer (400 MHz for ^{1}H and 100 MHz for ^{13}C) with a broad band probe at 20 ± 0.5 °C using methanol-d_4 (Cambridge Isotope Laboratories, Inc.) as the solvent. HRESIMS spectra were collected on an Agilent 6538 ultra high definition Accurate-Mass Q-TOF system. The LC-MS data were acquired on a Shimadzu UFLC coupled to a quadrupole mass spectrometer using a Phenomenex Kinetex C_{18} column (3.0 mm × 75 mm, 2.6 μm particle size) and MeCN–H_2O (with 0.1% HCOOH) gradient (1:9 to 0:10 in 12 min) followed by a 100% MeCN wash. Column chromatography was conducted using silica gel 60 (40–63 μm particle size) and Sephadex LH-20. TLC silica gel 60 F_{254} plates from EMD Chemicals Inc. were used for TLC. Separations were also carried out using a Shimadzu HPLC system equipped with LC-6AD solvent delivery pumps coupled to an SPD-10AV UV–vis detector or a Waters system equipped with a 1525 binary HPLC pump coupled to a 2998 PDAD detector. Both systems utilized Phenomenex C_{18} columns (21.2 × 250 mm or 10 × 250 mm, 5 μm particle size) for preparative runs. X-ray diffraction data for compound **7** were collected using a diffractometer with a Bruker APEX ccd area detector and graphite-monochromated Mo Kα radiation (λ = 0.710 73 Å). All solvents were of ACS grade or better.

Fungal Isolate Procurement and Culture Conditions. A soil sample was collected from beneath a granite monument on the grounds of one of the author's (J.B.K.) family property in Buffalo Valley, Oklahoma. The sample was processed using the method described by Du et al.,[9] and 51 fungal isolates were purified. Isolate BVK-SMA-2 was obtained on a starch-milk agar plate. The large-ribosomal-subunit internal transcribed spacer 1 (ITS1) region of the rDNA gene was sequenced at the Laboratory for Genomics and Bioinformatics, OU Health Sciences Center. Sequence data for the isolate (GenBank accession KM000126) was compared by BLAST analysis to sequences publicly available through the NCBI database.

For the 1 L Erlenmeyer flask cultures, an 80 mL volume of Cheerios breakfast cereal was added to each flask, and the flasks were autoclaved using a solid-cycle at 121 °C for 30 min. After the flasks were cooled to room temperature, a 48 mL aliquot of autoclaved 0.3% sucrose with 0.005% chloramphenicol was pipetted into the flasks to rehydrate the cereal. One ~5 mm × 5 mm chunk of the fungal isolate grown on an agar plate was added to each flask, and the cultures were incubated for 4 weeks.

When mycobags were used as the fermentation vessels, Cheerios breakfast cereal was preautoclaved using a solid-cycle at 121 °C for 30 min. After cooling, a 500 mL volume of Cheerios was added to each bag, the openings of the bags were folded over once, the folds were sealed with clamps, and bags were autoclaved using a liquid-cycle at 121 °C for 30 min. Eighteen ~5 mm × 5 mm chunks of fungal culture grown on an agar plate were prepared and mixed with the cereal. The cereal was then rehydrated with 850 mL of an autoclaved solution consisting of 0.3% sucrose with 0.005% chloramphenicol. The bags were placed flat to facilitate the formation of a monolayer of Cheerios across the bottom of the bag, and the cultures were incubated for 4 weeks.

Extraction and Compound Purification. The cultures were homogenized and extracted with EtOAc. The EtOAc extract (53.8 g) was subjected to silica gel flash chromatography with elution carried out using a step gradient of hexane–EtOAc (100:0, 50:50, 0:100) and EtOAc–MeOH (50:50, 0:100) to yield five fractions. Bioassay analysis of the resulting fractions revealed all of the biofilm inhibition activity was retained in fraction 4 (Fr.4). Accordingly, Fr.4 (EtOAc–MeOH, 50:50, 4.6 g) was subjected to Sephadex LH-20 column chromatography and eluted with MeOH–DCM (1:1), providing 16 subfractions. Recombination of the 16 fractions based on their TLC profiles yielded four subfractions (Fr.4-1–4-4). Fr.4-2 (0.9 g) was the only fraction exhibiting biofilm inhibition. Further purification of its components using C_{18} HPLC (250 mm × 20.2 mm, 5 μm) with a MeOH–H_2O gradient (from 80:20 to 100:0), as well as isocratic C_{18} HPLC (250 mm × 10 mm, 5 μm) with MeCN–H_2O containing 0.1% HCOOH (55:45, 72:28, or 78:22), yielded four known [TMC-151 C–F (**1**–**4**)] and three new polyketide glycosides [**5** (3 mg), **6** (12 mg), and **7** (4 mg)].

Base Hydrolysis of 6. A 1 mL aliquot of 0.4 M NaOH was added to **6** (10 mg), and the mixture was stirred at room temperature for 2 h. After the reaction mixture was neutralized with 1 M HCl, 1 mL of water was added and the mixture was partitioned with EtOAc (5 × 3 mL). The pooled EtOAc layers were reduced under vacuum to yield **7** (7.4 mg). The water layer was dried under vacuum and acetylated as described in the following section.

Acetylation of Mannitol. The solid product from the water layer was dissolved in 800 μL of anhydrous pyridine with 200 μL of acetic anhydride. The mixture was stirred at room temperature for 2 h. When the reaction was completed, 5 mL of EtOAc was added and the

Table 3. *In Vitro* Interaction between Amphotericin B and Compounds 1–7 Using the Checkerboard Method

	amphotericin B [A, μM (μg/mL)]			compound [B, μM (μg/mL)]			
compound	MIC[a] $_{single}$	MIC $_{combination}$	FIC $_A$	MIC $_{single}$	MIC $_{combination}$	FIC $_B$	FICI[b]
1	5 (4.6)	1.25 (1.15)	0.25	>100 (81)	5 (4)	<0.05	<0.30 S[c]
2	5 (4.6)	1.25 (1.15)	0.25	>100 (78)	1.25 (1)	<0.01	<0.26 S
3	5 (4.6)	1.25 (1.15)	0.25	50 (42)	1.25 (1.1)	0.03	0.28 S
4	5 (4.6)	1.25 (1.15)	0.25	50 (41)	1.25 (1.1)	0.03	0.28 S
5	5 (4.6)	1.25 (1.15)	0.25	>100 (60)	5 (3)	<0.05	<0.30 S
6	5 (4.6)	1.25 (1.15)	0.25	50 (45)	1.25 (1.1)	0.03	0.28 S
7	5 (4.6)	1.25 (1.15)	0.25	>100 (70)	5 (3.5)	<0.05	<0.30 S

[a]The MIC was defined as the lowest concentration causing prominent growth reduction (≥80% reduction in the metabolic activity). [b]FICI = FIC_A + FIC_B = ($MIC_{A\ combination}/MIC_{A\ single}$) + ($MIC_{B\ combination}/MIC_{B\ single}$). [c]S, synergistic interaction when FICI ≤ 0.5.

dx.doi.org/10.1021/np500531j | J. Nat. Prod. 2014, 77, 2273–2279

solution was washed repeatedly with H_2O (5 × 2 mL). The EtOAc layer was reduced under vacuum to yield **8** (4.3 mg).

Acid Methanolysis of 7. A solution of 1 M methanolic HCl (800 μL) was added to **7** (3.7 mg), and the solution was refluxed at 70 °C for 1.5 h. After the reaction mixture was neutralized with 1 M NaOH, 1 mL of water was added, and the solution was partitioned against EtOAc (5 × 3 mL). The water layer was evaporated under vacuum to provide **9** (~1.0 mg).

Single-Crystal X-ray Diffraction Analysis of 7. A colorless prism-shaped crystal of dimensions 0.420 × 0.230 × 0.100 mm was selected for structural analysis. The sample was cooled to 100 K. Cell parameters were determined from a nonlinear least-squares fit of 2682 peaks in the range $2.26° < \theta < 17.05°$. A total of 20 189 data were measured in the range $1.129° < \theta < 19.780°$ using ω oscillation frames. The data were corrected for absorption by the empirical method, giving minimum and maximum transmission factors of 0.963 and 0.991. The data were merged to form a set of 4239 independent data with $R(\text{int}) = 0.1301$ and a coverage of 50.9%. The monoclinic space group $C2$ was determined by systematic absences and statistical tests and verified by subsequent refinement. The structure was solved by direct methods and refined by full-matrix least-squares methods on F^2.[19] Positions of hydrogens bonded to carbons were initially determined by geometry and refined by a riding model. Hydrogens bonded to oxygen atoms were located on difference maps and were refined with a riding model. Non-hydrogen atoms were refined with anisotropic displacement parameters. Hydrogen atom displacement parameters were set to 1.2 (1.5 for methyl) times the displacement parameters of the bonded atoms. A total of 489 parameters were refined against 210 restraints and 4239 data to give $wR(F^2) = 0.4094$ and $S = 1.142$ for weights of $w = 1/[\sigma^2(F^2) + (0.1400P)^2 + 80.00P]$, where $P = [F_o^2 + 2F_c^2]/3$. The final $R(F)$ was 0.1647 for the 3058 observed $[F > 4\sigma(F)]$ data. The largest shift/s.u. was 0.036 in the final refinement cycle. The final difference map had maxima and minima of 0.889 and −0.427 e/Å^3, respectively. The polar axis restraint was taken from Flack and Schwarzenbach.[20] The intensity data were truncated to 1.05 Å resolution because data in higher resolution shells all had $\langle I/\sigma(I)\rangle < 2.0$. Atoms O10′ and C6′ were disordered (the occupancies for these atoms refined to 0.53[19] and 0.47[19] for the two structures illustrated in Figure S31). Restraints on the positional parameters of the disordered atoms and the displacement parameters of all atoms were required. Disordered solvent was also present and was accounted for using Babinet's principle.[21] The X-ray crystallographic data of **8** have been deposited in the Cambridge Crystallographic Data Center under accession number CCDC 1007026. The data can be accessed free of charge at http://www.ccdc.cam.ac.uk/.

Assays for *C. albicans* Growth Inhibition and Disruption of Biofilm Formation. The *C. albicans* strain SC5314 was cultured in brain heart infusion medium (BHI medium, Becton Dickinson) or RPMI-1640 plus MOPS medium [RPMI-1640 medium (Sigma) buffered to pH 7.0 with 0.17 M MOPS 3-(*N*-morpholino)-propanesulfonic acid (Sigma)] as required. The effects of compounds on the growth of *C. albicans* were tested using the method described in the NCCLS 2008 CLSI M27-A3 guidelines. The biofilm assay was performed as described with the following modifications. Cells of *C. albicans* SC5314 were cultured in BHI medium (Becton Dickinson) at 37 °C overnight. The cells were pelleted by centrifugation, washed with sterile PBS (phosphate-buffered saline, pH 7.4), and resuspended in RPMI-1640 plus MOPS medium. Test compounds were prepared in DMSO at stock concentrations of 20 mM before being serially diluted in RPMI-1640 plus MOPS medium for testing. ETYA was used as a positive control.[7] Aliquots of yeast suspension (100 μL containing 2.5×10^3 cells mL^{-1}) were added to the medium containing the diluted compounds or DMSO [final concentrations did not exceed 1% (v/v)] before being transferred to 96-well plates (Corning). After 48 h of incubation at 37 °C, the viability of the yeast was measured using the XTT assay. In brief, yeast cells were treated with 0.1 mg mL^{-1} XTT at 37 °C for 1 h. Absorbance measurements were taken at 492 nm using a microplate reader (Infinite M200). The minimum inhibitory concentrations (MIC) were defined as the lowest antifungal concentrations that caused ≥80% reduction in metabolic activity.

For determining the inhibition of biofilm formation, the medium was removed by aspiration from cells that were actively growing in microtiter plates, and the wells were washed twice with sterile PBS to remove nonadherent cells. Fresh medium (100 μL RPMI-1640 plus MOPS) was then added back to each well. Biofilm formation was measured using the XTT assay. All experiments were performed in triplicate on three separate occasions. The 50% inhibitory concentration values (IC_{50}) for biofilm formation inhibition were calculated using GraphPad Prism 5. The effects of compounds on biofilm formation were confirmed by fluorescence microscopy (Operetta, PerkinElmer). After washing with PBS, yeasts were stained with Calcofluor white and held at 37 °C for 10 min.

Checkerboard Assay for Synergistic Activity. To evaluate the synergistic effects of compound **1**−**7** with amphotericin B, a checkerboard assay was used.[22] *C. albicans* cells were seeded in 96-well plates and treated with different concentrations of test compounds alone or in combination with amphotericin B in RPMI-1640 plus MOPS medium at 37 °C for 48 h. The viability of the yeast was measured using the XTT assay, and the MIC for growth was defined as the lowest antifungal concentrations that caused ≥80% reduction in the metabolic activity. The interactions of test compounds with amphotericin B were determined according to the resultant FICI values. FICI values were calculated as follows: $\text{FICI} = \text{FIC}_A + \text{FIC}_B = (\text{MIC}_{A\ \text{combination}}/\text{MIC}_{A\ \text{single}}) + (\text{MIC}_{B\ \text{combination}}/\text{MIC}_{B\ \text{single}})$. The interpretation of the FICI data was determined as follows: ≤0.5, synergistic effect; >0.5 but <4, indifference (no effect); and ≥4, antagonistic effect.

*Bionectriol B (**5**):* colorless, amorphous solid; UV (MeOH) λ_{max} (log ε) 206 (4.31) nm; $[\alpha]_D^{25}$ +3 (*c* 0.24, MeOH); ^{1}H and ^{13}C NMR (see Table 1); HRESIMS *m*/*z* 625.3934 $[M + Na]^+$ (calcd for $C_{32}H_{58}O_{10}Na$, 625.3928).

*Bionectriol C (**6**):* colorless, amorphous solid; UV (MeOH) λ_{max} (log ε) 206 (4.27) nm; $[\alpha]_D^{25}$ +12 (*c* 0.26, MeOH); ^{1}H and ^{13}C NMR (see Table 1); HRESIMS *m*/*z* 929.5474 $[M + Na]^+$ (calcd for $C_{46}H_{82}O_{17}Na$, 929.5450).

*Bionectriol D (**7**):* colorless, prism-shaped crystals; UV (MeOH) λ_{max} (log ε) 206 (4.29) nm; $[\alpha]_D^{25}$ +7 (*c* 0.12, MeOH); ^{1}H and ^{13}C NMR (see Table 1); HRESIMS *m*/*z* 723.4667 $[M + Na]^+$ (calcd for $C_{38}H_{68}O_{11}Na$, 723.4659).

■ ASSOCIATED CONTENT

Ⓢ Supporting Information

1D and 2D NMR spectra and HRESIMS data for compounds **5**−**7** and 1D NMR spectra of **8** and **9** are available free of charge via the Internet at http://pubs.acs.org.

■ AUTHOR INFORMATION

Corresponding Author

*Tel: 1-405-325-6969. Fax: 1-405-325-6111. E-mail: rhcichewicz@ou.edu.

Author Contributions

§B. Wang and J. You contributed equally to this work.

Notes

The authors declare no competing financial interest.

■ ACKNOWLEDGMENTS

The reported research was supported by the National Institute of Allergy and Infectious Diseases of the National Institutes of Health under award number R01AI085161. The X-ray diffractometer was purchased through the National Science Foundation (CHE-0130835). We would like to thank Dr. A. Dongari-Bagtzoglou at the University of Connecticut Health Center for kindly providing the *C. albicans* SC5314 strain used in this study.

REFERENCES

(1) (a) Oral Candidiasis Statistics. Center for Disease Control and Prevention. Retrieved on August 12, 2013, from http://www.cdc.gov/fungal/diseases/candidiasis/thrush/statistics.html. (b) Genital/Vulvovaginal Candidiasis. Center for Disease Control and Prevention. Retrieved on August 12, 2013, from http://www.cdc.gov/fungal/diseases/candidiasis/genital/. (c) Invasive Candidiasis. Center for Disease Control and Prevention. Retrieved on August 12, 2013 from http://www.cdc.gov/fungal/diseases/candidiasis/invasive/.
(2) Douglas, L. J. *Trends Microbiol.* **2003**, *11*, 30−36.
(3) Harriott, M. M.; Lilly, E. A.; Rodriguez, T. E.; Fidel, P. L., Jr.; Noverr, M. C. *Microbiology* **2010**, *156*, 3635−3644.
(4) Finkel, J. S.; Mitchell, A. P. *Nat. Rev. Microbiol.* **2011**, *9*, 109−118.
(5) Wang, X.; You, J.; King, J. B.; Powell, D. R.; Cichewicz, R. H. *J. Nat. Prod.* **2012**, *75*, 707−715.
(6) Wang, X.; Du, L.; You, J.; King, J. B.; Cichewicz, R. H. *Org. Biomol. Chem.* **2012**, *10*, 2044−2050.
(7) You, J.; Du, L.; King, J. B.; Hall, B. E.; Cichewica, R. H. *ACS Chem. Biol.* **2013**, *8*, 840−848.
(8) Barrios-González, J. *Process Biochem.* **2012**, *47*, 175−185.
(9) Du, L.; King, J. B.; Morrow, B. H.; Shen, J. K.; Miller, A. N.; Cichewicz, R. H. *J. Nat. Prod.* **2012**, *75*, 1819−1823.
(10) Cai, S.; Du, L.; Gerea, A. L.; King, J. B.; You, J.; Cichewicz, R. H. *Org. Lett.* **2013**, *15*, 4186−4189.
(11) Kohno, J.; Nishio, M.; Sakurai, M.; Kawano, K.; Hiramatsu, H.; Kameda, N.; Kishi, N.; Yamashita, T.; Okuda, T.; Komatsubara, S. *Tetrahedron* **1999**, *55*, 7771−7786.
(12) Ju, Y.-M.; Juang, S.-H.; Chen, K.-J.; Lee, T.-H. *Z. Naturforsch.* **2007**, *62b*, 561−564.
(13) Freinkman, E.; Oh, D.-C.; Scott, J. J.; Currie, C. R.; Clardy, J. *Tetrahedron Lett.* **2009**, *50*, 6834−6837.
(14) Tomoda, H.; Tabata, N.; Ohyama, Y.; Ōmura, S. *J. Antibiot.* **2003**, *56*, 24−29.
(15) Tabata, N.; Ohyama, Y.; Tomoda, H.; Abe, T.; Namikoshi, M.; Ōmura, S. *J. Antibiot.* **1999**, *52*, 815−826.
(16) Kasai, Y.; Komatsu, K.; Shigemori, H.; Tsuda, M.; Mikami, Y.; Kobayashi, J. *J. Nat. Prod.* **2005**, *68*, 777−779.
(17) Kasai, R.; Okihara, M.; Asakawa, J.; Mizutani, K.; Tanaka, O. *Tetrahedron* **1979**, *35*, 1427−1432.
(18) Pei, Y.-H.; Hua, H.-M.; Li, Z.-L.; Chen, G. *Acta Pharm. Sin.* **2011**, *46*, 127−131.
(19) Sheldrick, G. M. *SHELXL*; Georg-August-Universität Göttingen, Germany, 2014.
(20) Flack, H. D.; Schwarzenbach, D. *Acta Crystallogr.* **1988**, *A44*, 499−506.
(21) Moews, P. C.; Kretsinger, R. H. *J. Mol. Biol.* **1975**, *91*, 201−225.
(22) Vitale, R. G.; Afeltra, J.; Dannaoui, E. *Methods Mol. Med.* **2005**, *118*, 143−152.